

Position Paper: An Integrated Perspective on Data, Metrics, and Methodology for Deep Time-Series Forecasting

Jiawen Zhang^{*1} Xumeng Wen² Shun Zheng² Jia Li¹ Jiang Bian²

Abstract

Deep time-series forecasting plays an integral role in numerous practical applications. However, existing research fall short by focusing narrowly on either neural architecture designs for long-term point forecasts or probabilistic models for short-term scenarios. By proposing a comprehensive framework, facilitated by a novel tool, ProbTS, that integrates diverse data scenarios, evaluation metrics, and methodological focuses, we aim to transcend the limitations of current forecasting practices. Rigorous experimentation uncovers pivotal insights, including the supreme importance of aligning forecasting methodologies with the unique characteristics of the data; the necessity of a broad spectrum of metrics for accurately assessing both point and distributional forecasts; and the challenges inherent in adapting existing forecasting methods to a wider range of scenarios. These findings not only challenge conventional approaches but also illuminate promising avenues for future research, suggesting a more nuanced and effective strategy for advancing the field of deep time-series forecasting.¹

1. Introduction

Deep time-series forecasting serves a crucial role in a myriad of practical applications, from traffic flow forecasting (Lv et al., 2014) and renewable energy forecasting (Wang et al., 2019), to diverse forecasting demands in retail (Böse et al., 2017), finance (Hou et al., 2021), and climate (Mudelsee, 2019). Each of these domains presents unique data characteristics, such as trend movements (Taylor & Letham, 2018), periodic patterns (Smyl, 2020), complicated mixtures of global seasonality and local variations (Fan et al.,

^{*}This work was done during the internship at Microsoft Research Asia, Beijing, China. ¹HKUST(GZ), Guangzhou, China ²Microsoft Research Asia, Beijing, China. Jiawen Zhang <jzhang302@connect.hkust-gz.edu.cn>, Shun Zheng <shun.zheng@microsoft.com>.

¹The ProbTS tool will be open-sourced.

2022), as well as intricate distributional dependencies (Rasul et al., 2021b). These data characteristics collectively pose substantial challenges for accurate forecasting, and thereby necessitate the development of sophisticated modeling designs. In addition to accurate point forecasts, modern decision-making processes often require robust distributional forecasts to effectively manage uncertainty (Gneiting & Katzfuss, 2014; Hyndman & Athanasopoulos, 2018). These collective requirements emphasize the significance for methodologies that are not only versatile across various forecasting scenarios but also capable of delivering both point and distributional forecasts with high fidelity.

However, these practical needs also highlight a distinct gap in existing research for deep time-series forecasting, which tends to bifurcate into two streams: one focusing on neural architecture designs optimized for point forecasting in long-term scenarios, and the other on advancing probabilistic forecasting, primarily in short-term situations.

Particularly, one stream of research, exemplified by studies such as (Zhou et al., 2021; Wu et al., 2021; Liu et al., 2022; Zhang et al., 2022; Challu et al., 2023; Wu et al., 2023; Nie et al., 2023), primarily explores neural architecture designs tailored for time-series forecasting. These studies, however, mostly focused on point forecasts, and their architectural designs are largely driven by long-term forecasting scenarios that exhibit strong trending and seasonal patterns. Therefore, it remains unclear how these advancements in neural architecture designs can be effectively extended to distributional forecasts, and whether their specialized designs, which are closely tied to certain data patterns, maintain their effectiveness across varied data scenarios.

On the other hand, another line of research, including works like (Rasul et al., 2021b;a; Tashiro et al., 2021; Bilos et al., 2023; Kolloviev et al., 2023), emphasizes the adaption of deep generative modeling (Dinh et al., 2017; Papamakarios et al., 2017; Ho et al., 2020) to probabilistic time-series forecasting. Despite significant progress in characterizing complex data distributions without the need for a predefined closed-form prior distribution such as Gaussian (Salinas et al., 2019), these probabilistic models have primarily been developed and evaluated in short-term forecasting scenarios. Hence, it remains to be seen whether these designs can

be effectively transitioned to long-term forecasting, and whether improvements in distributional forecasts also yield benefits in point forecasts, especially when compared to the tailored architectural designs mentioned earlier.

In a bid to systematically bridge this research gap, in this paper, we propose a holistic framework that integrates diverse data scenarios, comprehensive evaluation metrics, and methodological innovations. This approach enables a nuanced analysis of why certain forecasting methodologies outperform others in specific contexts and how they could be optimized to improve both point and distributional forecasting. To be more concrete, firstly, in terms of data, we encompass various data scenarios, spanning different domains and forecasting horizons. More significantly, we aim to quantify key data characteristics, elucidating why certain methodological choices converge or diverge. Secondly, concerning metrics, we adopt a comprehensive set of evaluation strategies, assessing the performance of both point and distributional forecasts. Lastly, we revisit a selection of representative studies from different research branches, affirming their advancements in specific methodological focuses and examining their performance in seldom evaluated scenarios. Through this integrated lens, we aspire to illuminate previously unaddressed questions, expose overlooked limitations of existing methods in certain situations, and reveal our novel findings that could potentially open up new avenues for future research.

To achieve these ends, we develop a tool, `ProbTS`, which incorporates customized data, evaluation, and model modules in alignment with the integrated perspective. Rigorous experimentation with this tool has led us to a number of intriguing insights, which are concisely presented below and explored in greater detail in Section 4.

Firstly, regarding the data, we have discovered that *the distinctive characteristics of data in different forecasting scenarios primarily dictate the selection of methodology*. We have identified several fundamental indicators that assist in distinguishing the distinct needs of diverse forecasting scenarios, such as data from various domains, short-term versus long-term forecasting, and point versus distributional forecasting. Notably, these indicators also facilitate our understanding of why certain methodological choices align or diverge in particular cases.

Secondly, concerning metrics, we have discerned that *the use of a comprehensive suite of metrics is critical for both point and distributional forecasts*. This conclusion stems from our observation that optimal performance in distributional metrics does not necessarily translate to optimal performance in point forecasts, and vice versa. Importantly, this suggests that focusing solely on optimizing one type of evaluation objective could result in sub-optimal performance according to other evaluation criteria.

Thirdly, in relation to the first research branch primarily dedicated to developing new architectures tailored for long-term point forecasting scenarios, we have recognized *significant challenges and unresolved questions when adapting them to new scenarios, particularly those with distributional or short-term requirements*. The integration of these architectures with advanced distribution estimation capabilities remains an open issue. Furthermore, the advantages of specific designs created for long-term scenarios diminish significantly in short-term cases. Another interesting observation is that all these methods consistently favor non-autoregressive decoding schemes over their autoregressive counterparts for multi-step forecasting, likely due to the pronounced trends in many long-term forecasting scenarios.

In terms of the second research branch, which focuses on developing advanced probabilistic forecasting capabilities, primarily in short-term scenarios, we have observed that *extending existing probabilistic models to long-term scenarios presents significant challenges*. Specifically, they often underperform those point forecasting methods even in producing distributional forecasts. Different from the first branch, these probabilistic methods exhibit a balanced preference for autoregressive and non-autoregressive decoding schemes. Our analyses reveal that autoregressive probabilistic methods tend to propagate more errors as the forecasting horizon increases, and non-autoregressive probabilistic methods demand substantial computational resources, both in terms of memory and time, as the forecasting horizon expands significantly. Interestingly, we also discovered that autoregressive probabilistic methods exhibit significant advantages in dealing with strong seasonality, even in long-term forecasting scenarios. This suggests that autoregressive decoding holds substantial potential for long-term forecasting, provided we can effectively mitigate the error-propagation effect amplified by pronounced trending.

Lastly, by leveraging our versatile tool that facilitates a deeper understanding of the interplay between data characteristics, forecasting performance, and methodological choices, we underscore several under-explored yet valuable directions that not only illuminate the path forward for academic research but also hold profound implications for practical applications in a multitude of sectors.

2. Related Work

As outlined in the introduction, deep time-series forecasting can be divided into two primary branches. This section provides a more thorough review of these branches, as well as a brief overview of existing forecasting toolkits. Besides, we include a refined comparison in Appendix A.1.

Neural Architecture Designs in Time-series Forecasting. Significant research efforts have been devoted to improv-

ing neural architecture designs for time-series forecasting, with contributions ranging from extensions of multi-layer perceptrons (Oreshkin et al., 2020; Zhang et al., 2022) to customized recurrent or convolutional neural networks (Lai et al., 2018; LIU et al., 2022), and Transformer-based variants (Vaswani et al., 2017; Zhou et al., 2022). These studies typically employ non-autoregressive decoding schemes and focus on long-term forecasting scenarios, often characterized by strong trend and seasonality patterns. However, they predominantly limit themselves to point forecasts, capturing only the average future variations. While approaches like quantile regression (Wen et al., 2017; Lim et al., 2021) can mitigate this limitation, they still cannot replace the inherent capture of the data distribution.

Probabilistic Estimation in Time-series Forecasting. In contrast, the second branch of research, known as *deep probabilistic time-series forecasting*, focuses on leveraging deep neural networks to capture the complex data distribution of future time series. These studies span from early approaches using pre-defined likelihood functions (Rangapuram et al., 2018; Salinas et al., 2020), to Gaussian copulas (Salinas et al., 2019; Drouin et al., 2022), and to more recent methods exploiting advanced deep generative models (Rasul et al., 2021b; Bilos et al., 2023). While providing probabilistic forecasts, they mainly evaluate short-term forecasting scenarios. Interestingly, unlike the first branch, this branch utilizes both autoregressive (Rasul et al., 2021b;a) and non-autoregressive (Tashiro et al., 2021; Bilos et al., 2023; Kolloviev et al., 2023) decoding schemes. Furthermore, this branch tends to use general neural architectures instead of customizing them. While a few methods (Tashiro et al., 2021; Li et al., 2022; Bergsma et al., 2022) incorporate customized network designs, more studies (de Bézenac et al., 2020; Rasul et al., 2021b;a; Bilos et al., 2023; Drouin et al., 2022) leverage standardized neural networks to encode time-series representations.

Toolkits for Time-series Forecasting. We observe a plethora of toolkits that have been developed for time-series forecasting. These range from those primarily designed for point forecasting, such as Prophet (Taylor & Letham, 2018), sktime (Löning et al., 2019), tsai (Oguiza, 2022), and TSLib (Wu et al., 2023), to others that incorporate probabilistic forecasting, including GluonTS (Alexandrov et al., 2020), PyTorchTS (Rasul et al., 2021b), PyTorchForecasting², and NeuralForecast³. In the development of ProbTS, we drew upon these existing tools, particularly PyTorchTS and GluonTS. However, ProbTS distinguishes itself by its specialized design towards the integrated perspective proposed in this paper, encompassing modularized designs

across data, methodology, and evaluation components. Furthermore, we incorporate more state-of-the-art forecasting models in ProbTS, by migrating their official implementations and conducting extensive hyper-parameter tuning to ensure optimal performance.

3. The ProbTS Tool

This section offers a concise overview of the ProbTS tool’s design and implementation. The core modules and the primary pipeline of ProbTS are depicted in Figure 1.

Data. We aggregate publicly accessible datasets used for both short-term and long-term forecasting. Initial data visualization analyses reveal that the data domains and forecasting horizons significantly influence specific data characteristics within a given forecasting horizon. For instance, many long-term forecasting scenarios exhibit clear trend and seasonality patterns within a forecasting window, while numerous short-term forecasting cases display irregular variations within a short sliding window. Consequently, we have developed quantified indicators, such as trend and seasonality strengths, along with *non-Gaussianity* to indicate the complexity of data distribution within a forecasting window. Detailed information about dataset statistics, visualization analyses, and quantified measures can be found in Appendix A.2, A.3, A.4, and A.5. The quantified measurements for all forecasting scenarios are compiled in Table 1.

Metrics. ProbTS incorporates a broad range of evaluation metrics to enable a thorough assessment of both point and distributional forecasts. These metrics are elaborated in detail in Appendix A.6. In this paper, we primarily use the normalized mean absolute error (NMAE) for point forecasts and the continuous ranked probability score (CRPS) for distributional forecasts to succinctly communicate the critical insights discovered. It is noteworthy that some methods reproduced in ProbTS, their original papers reported certain point forecast metrics before de-normalizing forecasts to the initial scale (Zeng et al., 2023; Wu et al., 2023; Nie et al., 2023) or primarily reveal aggregated distributional metrics over all time-series variates, namely CRPS-sum (Salinas et al., 2019; Rasul et al., 2021a;b). We have diligently ensured our reproduced results align with their reported results and utilized the unified metrics in this study to offer a comprehensive and fair comparison.

Model. The design of our model module is modularized to accommodate various methodological focuses, such as point versus distributional forecasts, customized versus general neural architectures for encoding time-series representations, and autoregressive versus non-autoregressive decoding schemes. This design enables us to easily integrate with existing methods by selecting different routes and con-

²github.com/jdb78/pytorch-forecasting

³github.com/Nixtla/neuralforecast

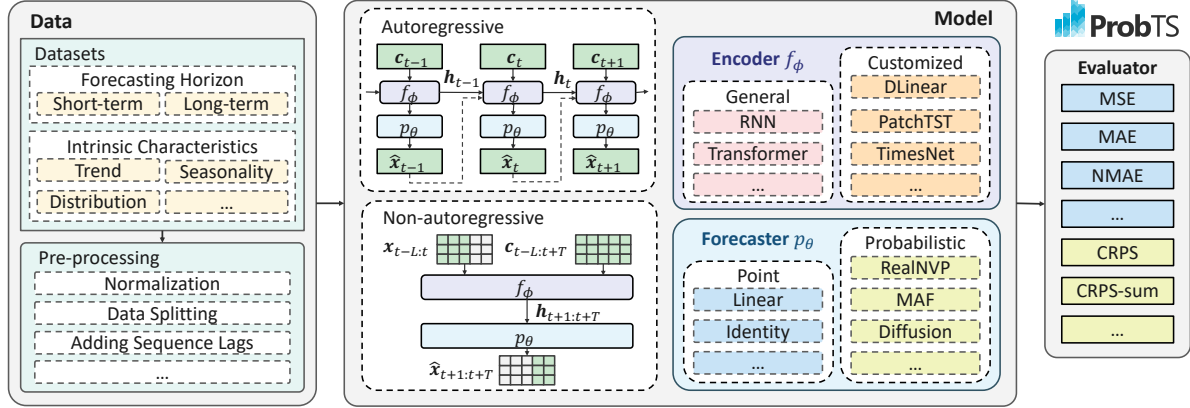


Figure 1. An overview of ProbTS.

figuring specific components appropriately. Specifically, our design is grounded on the following formulation for time-series forecasting that considers different forecasting paradigms and decoding schemes.

Formulation. We denote an element of a multivariate time series as $x_t^k \in \mathbb{R}$, where k represents the variate index and t denotes the time index. At time step t , we have a multivariate vector $\mathbf{x}_t \in \mathbb{R}^K$. Each x_t^k is associated with covariates $\mathbf{c}_t^k \in \mathbb{R}^N$, which encapsulates auxiliary information about the observations. Given a length- T forecast horizon a length- L observation history $\mathbf{x}_{t-L:t}$ and corresponding covariates $\mathbf{c}_{t-L:t}$, the objective in time series forecasting is to generate the vector of future values $\mathbf{x}_{t+1:t+T}$. In ProbTS, we decouple a model into an encoder f_ϕ and a forecaster p_θ . An encoder is tasked with generating expressive hidden states $\mathbf{h} \in \mathbb{R}^D$. Under *autoregressive* decoding scheme, encoder forecasts variates using their past values, which can be formulated as $\mathbf{h}_t = f_\phi(\mathbf{x}_{t-1}, \mathbf{c}_t, \mathbf{h}_{t-1})$. Under the *non-autoregressive* scheme, the encoder generates all the forecasts in one step, which can be expressed as $\mathbf{h}_{t+1:t+T} = f_\phi(\mathbf{x}_{t-L:t}, \mathbf{c}_{t-L:t+T})$. A forecaster p_θ is employed either to directly estimate *point forecasts* as $\hat{\mathbf{x}}_t = p_\theta(\mathbf{h}_t)$, or to perform sampling based on the estimated *probabilistic distributions* as $\hat{\mathbf{x}}_t \sim p_\theta(\mathbf{x}_t | \mathbf{h}_t)$.

4. Analyses

Utilizing ProbTS, we benchmarked selected methods in both short-term and long-term forecasting scenarios. We evaluated these methods using both point and distributional forecast metrics. To ensure the reliability of our results and minimize randomness, we performed each experiment five times with different seeds for parameter initialization. The results for short-term and long-term forecasting are presented in Table 2 and Table 3, respectively.

Selected Methods for Comparison. We have chosen representative methods from various research branches for comparison. Our selection is based on a comprehensive consideration of factors such as state-of-the-art performance, reproducibility, as well as the simplicity, universality, and novelty of the method designs. Adhering to these principles, we have selected PatchTST (Nie et al., 2023), TimesNet (Wu et al., 2023), N-HiTS (Challu et al., 2023), LTSF-Linear (NLinear and DLinear) (Zeng et al., 2023) from the research line that concentrates on developing customized neural architectures for long-term point forecasting. In addition, we have chosen advanced probabilistic forecasting methods for comparison, including those built upon normalizing flows such as GRU NVP, GRU MAF, and Trans MAF (Rasul et al., 2021b), and diffusion models such as TimeGrad (Rasul et al., 2021a) and CSDI (Tashiro et al., 2021). We also include general network architectures, such as Linear, GRU (Chung et al., 2014), and Transformer (Vaswani et al., 2017), to demonstrate the additional benefits brought by advanced architecture designs or probabilistic estimations. Simple non-parametric baselines, such as calculating the global mean or batch mean as all forecasts, are also included to assess the predictability of a forecasting scenario.

4.1. Discrepancies in Point and Distributional Metrics.

Our analysis revealed that optimal performance in distributional metrics does not guarantee optimal performance in point forecasts. This pattern emerged in several instances, notably in Table 3. For example, CSDI excels in the CRPS metric but falls short in NMAE across multiple datasets, such as ETTm1, ETTm2, and ETTh2. These observations underscore the necessity of a comprehensive evaluation utilizing both NMAE and CRPS metrics to gain a holistic understanding of performance in both point and distributional forecasting. It is worth highlighting that these two metrics become equivalent for point forecasting methods

Table 1. This table presents a quantitative assessment of the inherent characteristics for all forecasting scenarios, each corresponding to a dataset with a specific forecasting horizon. We use the suffixes ”-S” and ”-L” to differentiate between short-term and long-term scenarios. Quantified indicators encompass trend and seasonality strengths, as well as non-Gaussianity, where a higher value signifies a greater deviation from a Gaussian distribution.

Dataset-Horizon	Exchange-S	Solar-S	Electricity-S	Traffic-S	Wikipedia-S	ETTm1-L	ETTm2-L
Trend	0.9982	0.1688	0.6443	0.2880	0.5253	0.9462	0.9770
Seasonality	0.1256	0.8592	0.8323	0.6656	0.2234	0.0105	0.0612
Non-Gaussianity	0.2967	0.5004	0.3579	0.2991	0.2751	0.0833	0.1701
Dataset-Horizon	ETTh1-L	ETTh2-L	Electricity-L	Traffic-L	Weather-L	Exchange-L	ILI-L
Trend	0.7728	0.9412	0.6476	0.1632	0.9612	0.9978	0.5438
Seasonality F_S	0.4772	0.3608	0.8344	0.6798	0.2657	0.1349	0.6075
Non-Gaussianity	0.0719	0.1422	0.1533	0.1378	0.1727	0.1082	0.1112

Table 2. Results (mean_{std}) on short-term forecasting scenarios, each containing five independent runs with different seeds.

Model	Exchange Rate		Solar		Electricity		Traffic		Wikipedia	
	CRPS	NMAE								
Glob. mean	0.188	0.188	1.403	1.403	0.412	0.412	0.540	0.540	0.577	0.577
Batch mean	0.012	0.012	1.244	1.244	0.365	0.365	0.503	0.503	0.336	0.336
Linear	0.012 _{.001}	0.012 _{.001}	0.704 _{.036}	0.704 _{.036}	0.138 _{.009}	0.138 _{.009}	0.327 _{.032}	0.327 _{.032}	0.874 _{.151}	0.874 _{.151}
GRU	0.013 _{.002}	0.013 _{.002}	0.594 _{.144}	0.594 _{.144}	0.134 _{.009}	0.134 _{.009}	0.193 _{.002}	0.193 _{.002}	0.394 _{.013}	0.394 _{.013}
Transformer	0.016 _{.001}	0.016 _{.001}	0.538 _{.066}	0.538 _{.066}	0.115 _{.005}	0.115 _{.005}	0.204 _{.006}	0.204 _{.006}	0.408 _{.011}	0.408 _{.011}
N-HiTS	0.012 _{.000}	0.012 _{.000}	0.572 _{.020}	0.572 _{.020}	0.074 _{.003}	0.074 _{.003}	0.193 _{.002}	0.193 _{.002}	0.332 _{.011}	0.332 _{.011}
NLinear	0.010 _{.000}	0.010_{.000}	0.560 _{.002}	0.560 _{.002}	0.083 _{.002}	0.083 _{.002}	0.233 _{.001}	0.233 _{.001}	0.321 _{.001}	0.321 _{.001}
DLinear	0.012 _{.001}	0.012 _{.001}	0.547 _{.009}	0.547 _{.009}	0.076 _{.003}	0.076 _{.003}	0.250 _{.002}	0.250 _{.002}	0.412 _{.001}	0.412 _{.001}
PatchTST	0.010 _{.000}	0.010_{.000}	0.496 _{.002}	0.496 _{.002}	0.067 _{.001}	0.067 _{.001}	0.202 _{.001}	0.202 _{.001}	0.257 _{.001}	0.257_{.001}
TimesNet	0.011 _{.001}	0.011 _{.001}	0.507 _{.019}	0.507 _{.019}	0.071 _{.002}	0.071 _{.002}	0.205 _{.002}	0.205 _{.002}	0.304 _{.002}	0.304 _{.002}
GRU NVP	0.016 _{.003}	0.020 _{.003}	0.396 _{.021}	0.507 _{.022}	0.055 _{.002}	0.073 _{.003}	0.161 _{.006}	0.203 _{.009}	0.282 _{.003}	0.330 _{.003}
GRU MAF	0.015 _{.001}	0.020 _{.001}	0.386 _{.026}	0.492 _{.027}	0.051 _{.001}	0.067 _{.001}	0.131 _{.006}	0.165 _{.009}	0.281 _{.004}	0.337 _{.005}
Trans MAF	0.011 _{.001}	0.014 _{.001}	0.400 _{.022}	0.503 _{.022}	0.054 _{.004}	0.071 _{.005}	0.129_{.004}	0.165_{.006}	0.289 _{.008}	0.344 _{.008}
TimeGrad	0.011 _{.001}	0.014 _{.002}	0.359_{.011}	0.445_{.023}	0.052 _{.001}	0.067 _{.001}	0.164 _{.091}	0.201 _{.115}	0.272 _{.008}	0.327 _{.011}
CSDI	0.008_{.000}	0.011 _{.000}	0.366 _{.005}	0.484 _{.008}	0.050_{.001}	0.065_{.001}	0.146 _{.012}	0.176 _{.013}	0.219_{.006}	0.259 _{.009}

when a point forecast is converted into a degenerate distribution, centered on the forecasted point, for CRPS evaluation (Gneiting & Raftery, 2007).

4.2. Examination of Customized Neural Architectures

Our findings affirm the progress in this area of research. For instance, as observed in Table 3, the state-of-the-art architecture, PatchTST, consistently surpasses other models, especially when assessed using the NMAE metric. The only exception is on the Traffic dataset, where PatchTST is outperformed by GRU NVP and TimeGrad. This discrepancy is primarily attributable to the different decoding schemes utilized, which will be elaborated in Section 4.3.

Diminishing Advantages of Customized Architectures in Short-term Forecasting Scenarios. Interestingly, the significant superiority of PatchTST diminishes in short-term

forecasting scenarios. This trend is evident when comparing Table 3 and 2. More intuitively, Figures 2a, 2c display the relative strengths of point and probabilistic forecasting methods in terms of NMAE, and correlates their NMAE values with our quantified indicator, non-Gaussianity, used for assessing data distribution complexity. We further observe that as non-Gaussianity increases, signifying a more complex data distribution, a noticeable performance gap emerges. This suggests that the reducing superiority of these customized architectures may be due to their limited capability to handle complex data distributions.

Challenges in Integrating Advanced Distribution Estimation Capabilities with These Architectures. Regrettably, the integration of these architectures with advanced distribution estimation capabilities remains a challenging task. As will be discussed subsequently, non-autoregressive probabilistic methods encounter significant efficiency issues in

Table 3. Results (mean_{std}) on long-term forecasting scenarios, each containing five independent runs with different seeds. The input sequence length is set to 36 for the ILI dataset and 96 for the others. Due to the excessive time and memory consumption of CSDI in producing long-term forecasts, its results are unavailable in some datasets.

Model	pred len	DLinear		PatchTST		GRU NVP		TimeGrad		CSDI	
		CRPS	NMAE	CRPS	NMAE	CRPS	NMAE	CRPS	NMAE	CRPS	NMAE
ETTm1	96	0.282.002	0.282.002	0.272.001	0.272.001	0.383.053	0.488.058	0.522.105	0.645.129	0.236.006	0.308.005
	192	0.309.004	0.309.004	0.295.001	0.295.001	0.396.030	0.514.042	0.603.092	0.748.084	0.291.025	0.377.026
	336	0.338.008	0.338.008	0.323.001	0.323.001	0.486.032	0.630.029	0.601.028	0.759.015	0.322.033	0.419.042
	720	0.387.006	0.387.006	0.353.001	0.353.001	0.546.036	0.707.050	0.621.037	0.793.034	0.448.038	0.578.051
ETTm2	96	0.138.000	0.138.000	0.132.001	0.132.001	0.319.044	0.413.059	0.427.042	0.525.047	0.115.009	0.146.012
	192	0.163.003	0.163.003	0.157.001	0.157.001	0.326.025	0.427.033	0.424.061	0.530.060	0.147.008	0.189.012
	336	0.188.001	0.188.001	0.176.000	0.176.000	0.449.145	0.580.169	0.469.049	0.566.047	0.190.018	0.248.024
	720	0.219.003	0.219.003	0.205.001	0.205.001	0.561.273	0.749.385	0.470.054	0.561.044	0.239.035	0.306.040
ETTh1	96	0.352.011	0.352.011	0.328.003	0.328.003	0.379.030	0.481.037	0.455.046	0.585.058	0.437.018	0.557.022
	192	0.393.001	0.393.001	0.359.002	0.359.002	0.425.019	0.531.018	0.516.038	0.680.058	0.496.051	0.625.065
	336	0.419.007	0.419.007	0.384.002	0.384.002	0.458.054	0.580.064	0.512.026	0.666.047	0.454.025	0.574.026
	720	0.502.029	0.502.029	0.397.002	0.397.002	0.502.039	0.643.046	0.523.027	0.672.015	0.528.012	0.657.014
ETTh2	96	0.211.027	0.211.027	0.177.000	0.177.000	0.432.141	0.548.158	0.358.026	0.448.031	0.164.013	0.214.018
	192	0.238.028	0.238.028	0.201.001	0.201.001	0.625.170	0.766.223	0.457.081	0.575.089	0.226.018	0.294.027
	336	0.284.008	0.284.008	0.240.001	0.240.001	0.793.319	0.942.408	0.481.078	0.606.095	0.274.022	0.353.028
	720	0.307.000	0.307.000	0.252.000	0.252.000	0.539.090	0.688.161	0.445.016	0.550.018	0.302.040	0.382.030
Electricity	96	0.090.001	0.090.001	0.086.001	0.086.001	0.094.003	0.118.003	0.096.002	0.119.003	0.153.137	0.203.189
	192	0.095.001	0.095.001	0.092.001	0.092.001	0.097.002	0.121.003	0.100.004	0.124.005	0.200.094	0.264.129
	336	0.104.000	0.104.000	0.100.000	0.100.000	0.099.001	0.123.001	0.102.007	0.126.008	-	-
	720	0.122.001	0.122.001	0.116.000	0.116.000	0.114.013	0.144.017	0.108.003	0.134.004	-	-
Traffic	96	0.356.009	0.356.009	0.248.001	0.248.001	0.187.002	0.231.003	0.202.004	0.234.006	-	-
	192	0.346.009	0.346.009	0.245.001	0.245.001	0.192.001	0.236.002	0.208.003	0.239.004	-	-
	336	0.350.008	0.350.008	0.257.002	0.257.002	0.201.004	0.248.006	0.213.003	0.246.003	-	-
	720	0.365.009	0.365.009	0.266.001	0.266.001	0.211.004	0.264.006	0.220.002	0.263.001	-	-
Weather	96	0.112.001	0.112.001	0.087.002	0.087.002	0.116.013	0.145.017	0.130.017	0.164.023	0.068.008	0.087.012
	192	0.122.001	0.122.001	0.090.001	0.090.001	0.122.021	0.147.025	0.127.019	0.158.024	0.068.006	0.086.007
	336	0.130.002	0.130.002	0.092.002	0.092.002	0.128.011	0.160.012	0.130.006	0.162.006	0.083.002	0.098.002
	720	0.144.001	0.144.001	0.094.001	0.094.001	0.110.004	0.135.008	0.113.011	0.136.020	0.087.003	0.102.005
Exchange	96	0.024.000	0.024.000	0.023.000	0.023.000	0.071.006	0.091.009	0.068.003	0.079.002	0.028.003	0.036.005
	192	0.035.000	0.035.000	0.034.000	0.034.000	0.068.004	0.087.005	0.087.013	0.100.019	0.045.003	0.058.005
	336	0.048.001	0.048.001	0.048.000	0.048.000	0.072.002	0.091.002	0.074.009	0.086.008	0.060.004	0.076.006
	720	0.075.002	0.075.002	0.072.000	0.072.000	0.079.009	0.103.009	0.099.015	0.113.016	0.143.020	0.173.020
ILI	24	0.213.038	0.213.038	0.169.005	0.169.005	0.257.003	0.283.001	0.275.047	0.296.044	0.250.013	0.263.012
	36	0.230.015	0.230.015	0.156.005	0.156.005	0.281.004	0.307.007	0.272.057	0.298.048	0.285.010	0.298.011
	48	0.221.009	0.221.009	0.156.008	0.156.008	0.288.008	0.314.009	0.295.033	0.320.025	0.285.036	0.301.034
	60	0.230.013	0.230.013	0.147.003	0.147.003	0.307.005	0.333.005	0.295.083	0.325.068	0.283.012	0.299.013

long-term forecasting. Intriguingly, all these architectures select a non-autoregressive decoding scheme. We will delve into the advantages and disadvantages of autoregressive and non-autoregressive schemes in the next section.

4.3. Assessment of Probabilistic Forecasting Methods

At the outset, we validate the efficacy of these probabilistic methods in the short-term forecasting scenarios they were designed for. Evidence from Table 2 demonstrates that innovative methods such as CSDI and TimeGrad yield superior results in most cases.

However, in Long-term Forecasting Scenarios, Probabilistic Methods Fall Short, Even When Evaluated Us-

ing Distributional Metrics. As depicted in Table 3, in a multitude of long-term forecasting scenarios, customized neural architectures, created specifically with point forecasting objectives in mind, decidedly outperform probabilistic methods, even when evaluated using distributional metrics such as CRPS. This suggests that existing probabilistic methods may encounter significant challenges when applied to long-term forecasting, leaving substantial room for improvement in this domain. To further illustrate this, we compare the CRPS performance of these models with the non-Gaussianity in both long-term and short-term scenarios, as depicted in Figure 2b and 2d, respectively. While non-Gaussianity does provide some insights—its values are relatively lower in long-term scenarios compared to short-term contexts—these explanations are not comprehensive. This

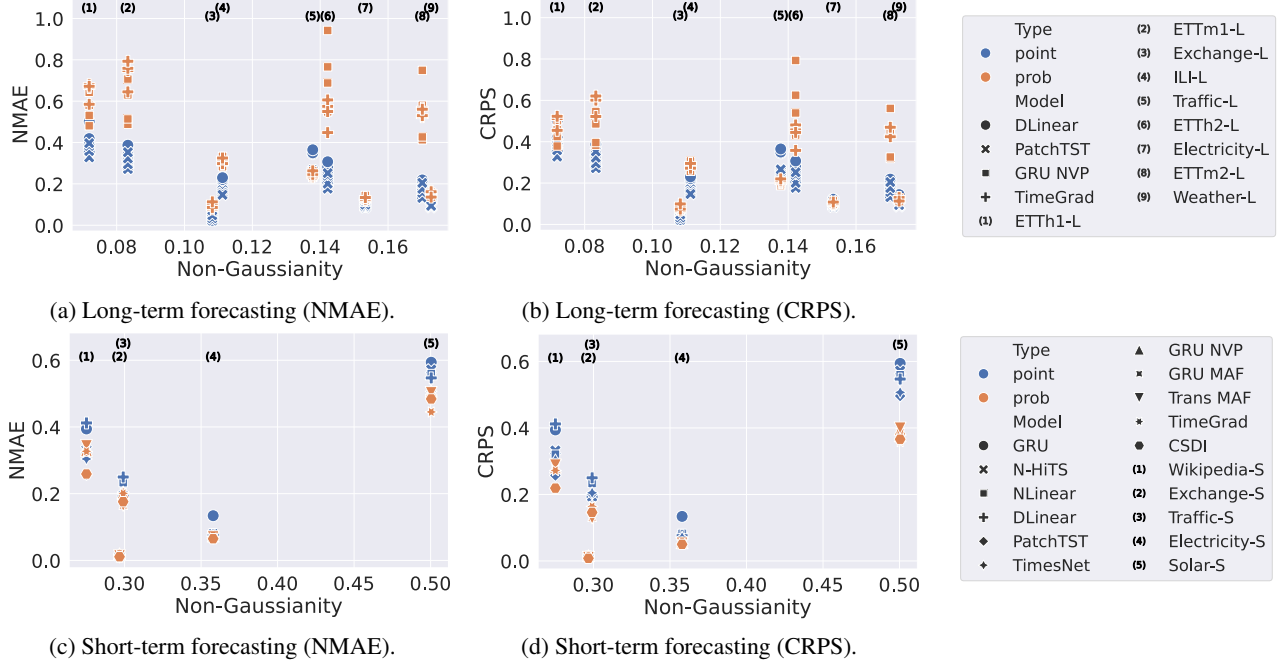


Figure 2. We present plots of the metrics against non-Gaussianity for various models across all forecasting scenarios. In each subplot, a vertical line of points represents one forecasting scenario, denoted by a sequence number at the top. We distinguish between point and probabilistic forecasting methods using different colors, and we use unique markers to indicate various models.

is because it remains unclear to what extent a customized neural model, coupled with effective probabilistic estimations, can perform. To delve deeper, we further examine other unique aspects of the existing probabilistic forecasting methods in search of potential clues.

The Dichotomy of Decoding Scheme Preferences. Upon further investigation, we find that these probabilistic forecasting methods exhibit a balanced preference for both autoregressive and non-autoregressive decoding schemes. For instance, TimeGrad employs an autoregressive decoding scheme, whereas CSDI utilizes a non-autoregressive decoding approach. This contrasts starkly with the aforementioned customized architectures, which solely opt for non-autoregressive decoding. These two types of decoding schemes, however, confront distinctive challenges when applied to long-term probabilistic forecasting.

- Autoregressive probabilistic methods, for example, TimeGrad, are prone to propagate more errors as the forecasting horizon increases or the trend strength enlarges. This phenomenon is evident in Figure 3a and 3b, where we observe that the performance gap escalates with either extended prediction lengths or intensified trend strengths.
- In contrast, non-autoregressive probabilistic methods, like CSDI, struggle with significant efficiency chal-

lenges, both in memory usage and time consumption, in long-term forecasting scenarios. This issue is further detailed in Appendix Section B.6. Furthermore, as indicated in Table 3, even for relatively small-scale datasets, such as ETTh2 and ETTh1, CSDI’s performance in long-term scenarios is less than optimal. This suggests that its learning efficacy is also compromised by the extension of the forecasting horizon.

The Unexpected Superiority of Autoregressive Decoding Scheme in Addressing Strong Seasonality. Interestingly, the autoregressive decoding scheme exhibits a remarkable proficiency in dealing with strong seasonality. A prime example is the results for the Traffic dataset shown in Table 3, where both GRU NVP and TimeGrad outperform PatchTST, despite utilizing relatively standard neural architectures without any customization. In Figure 3c, we further investigate this phenomenon by relating the strength of seasonality to the variance in performance gaps. Additionally, in Figure 3d, we conduct a collective analysis of the interactions among CRPS Gap, trend, and seasonality strengths, where the CRPS Gap is defined as the difference between the CRPS scores of TimeGrad (autoregressive) and CSDI (non-autoregressive). A clear pattern emerges: as the strength of seasonality heightens, autoregressive methods gain more advantages. This observation suggests that despite its challenges, the autoregressive decoding scheme should not be dismissed in long-term forecasting. Its unique

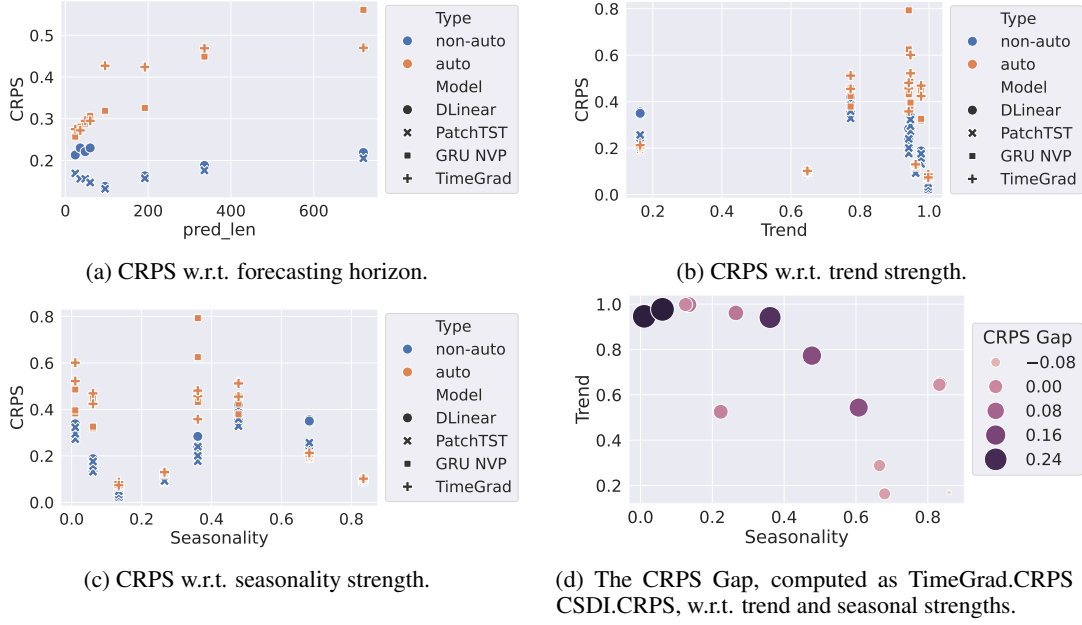


Figure 3. We analyze CRPS in relation to various factors to scrutinize the strengths and weaknesses of autoregressive probabilistic methods. Subplot (a), based on ETTm and ILI datasets, illustrates the error amplification that occurs with increased prediction length. Subplots (b) and (c) encompass all long-term forecasting scenarios, aiming to explore the relationship between CRPS and the strengths of trends and seasonality, respectively. Subplot (d) includes all forecasting scenarios, with a lighter and smaller circle denoting a preference for autoregressive methods over non-autoregressive ones.

affinity with seasonality, possibly due to superior parameter efficiency, may regain significance if we can develop effective strategies to mitigate the issue of error propagation.

4.4. Future Directions

Drawing on our analyses, we propose several promising directions for future research. Firstly, the development of hybrid learning objectives that optimize both point and distributional forecasts represents a significant advancement. This strategy could foster models capable of delivering more comprehensive predictions, catering to a diverse range of practical applications that necessitate both accurate predictions and well-quantified uncertainties. Secondly, there is an urgent need for the effective integration of neural architecture design with advanced probabilistic estimation paradigms. Addressing this demand could lay the groundwork for more efficient and precise forecasting models. Particularly, overcoming the efficiency challenges associated with non-autoregressive decoding schemes and reducing error propagation in autoregressive probabilistic models, specifically in the presence of marked trends, could substantially enhance the models' performance and practicality. Lastly, the exploration of the necessity and potential designs of customized architectures tailored for short-term forecasting could initiate a novel research field. Such exploration necessitates consideration of data characteristics beyond trends and seasonality.

4.5. Limitations

Despite the thoroughness of our study, there are several limitations. First, due to the vast number of methods available in this field, we could not include all of them in our analysis. Our selection is based on a set of criteria, but inevitably, some methods were left out. Second, while we have tried to incorporate a diverse range of datasets, there are certainly more datasets beyond those included in our study. To mitigate this limitation, we have conducted additional experiments on univariate time-series datasets, which are included in Appendix B.3. Finally, our study is primarily empirical in nature. While we have made significant efforts to conduct rigorous statistical analyses, we have not provided theoretical proofs for our results.

5. Conclusion

This paper presents an integrated perspective on data, metrics, and methodology in the field of deep time-series forecasting, facilitated by the ProbTS tool. Our findings not only provide valuable insights into the strengths and limitations of existing methods but also highlight several underexplored areas that merit future research. In addition, we expect that our insights could spur more explorations on these fields. We also hope the ProbTS tool can become a useful resource for the community, expediting future advancements in time-series forecasting.

Impact Statements

This paper presents work whose goal is to advance the field of Machine Learning. There are many potential societal consequences of our work, none which we feel must be specifically highlighted here.

References

Alexandrov, A., Benidis, K., Bohlke-Schneider, M., Flunkert, V., Gasthaus, J., Januschowski, T., Maddix, D. C., Rangapuram, S., Salinas, D., Schulz, J., Stella, L., Türkmen, A. C., and Wang, Y. GluonTS: Probabilistic and Neural Time Series Modeling in Python. *Journal of Machine Learning Research*, 21(116):1–6, 2020.

Athanasopoulos, G., Hyndman, R. J., Song, H., and Wu, D. C. The tourism forecasting competition. *International Journal of Forecasting*, 27(3):822–844, 2011.

Bergsma, S., Zeyl, T., Anaraki, J. R., and Guo, L. C2FAR: Coarse-to-Fine Autoregressive Networks for Precise Probabilistic Forecasting. In *In Proc. of NeurIPS*, 2022.

Bilos, M., Rasul, K., Schneider, A., Nevmyvaka, Y., and Günnemann, S. Modeling Temporal Data as Continuous Functions with Stochastic Process Diffusion. In *In Proc. of ICML*, pp. 2452–2470, 2023.

Böse, J.-H., Flunkert, V., Gasthaus, J., Januschowski, T., Lange, D., Salinas, D., Schelter, S., Seeger, M., and Wang, Y. Probabilistic demand forecasting at scale. *VLDB*, 2017.

Challu, C., Olivares, K. G., Oreshkin, B., Ramirez, F., Canseco, M., and Dubrawski, A. NHITS: Neural Hierarchical Interpolation for Time Series Forecasting. In *In Proc. of AAAI*, pp. 6989–6997, 2023.

Chung, J., Gülc̄ehre, Ç., Cho, K., and Bengio, Y. Empirical Evaluation of Gated Recurrent Neural Networks on Sequence Modeling. *CoRR*, abs/1412.3555, 2014.

de Bézenac, E., Rangapuram, S. S., Benidis, K., Bohlke-Schneider, M., Kurle, R., Stella, L., Hasson, H., Gallinari, P., and Januschowski, T. Normalizing Kalman Filters for Multivariate Time Series Analysis. In *In Proc. of NeurIPS*, pp. 2995–3007, 2020.

Dinh, L., Sohl-Dickstein, J., and Bengio, S. Density Estimation using Real NVP. In *In Proc. of ICLR*, 2017.

Drouin, A., Marcotte, E., and Chapados, N. TACTiS: Transformer-Attentional Copulas for Time Series. In *In Proc. of ICML*, pp. 5447–5493, 2022.

Elsayed, S., Thyssens, D., Rashed, A., Jomaa, H. S., and Schmidt-Thieme, L. Do we really need deep learning models for time series forecasting? *arXiv preprint arXiv:2101.02118*, 2021.

Falcon, W. and The PyTorch Lightning team. PyTorch Lightning, March 2019. URL <https://github.com/Lightning-AI/lightning>.

Fan, W., Zheng, S., Yi, X., Cao, W., Fu, Y., Bian, J., and Liu, T.-Y. DEPTS: Deep Expansion Learning for Periodic Time Series Forecasting. In *In Proc. of ICLR*, 2022.

Gneiting, T. and Katzfuss, M. Probabilistic forecasting. *Annual Review of Statistics and Its Application*, 2014.

Gneiting, T. and Raftery, A. E. Strictly Proper Scoring Rules, Prediction, and Estimation. *Journal of the American statistical Association*, 2007.

Ho, J., Jain, A., and Abbeel, P. Denoising Diffusion Probabilistic Models. In *In Proc. of NeurIPS*, 2020.

Hou, M., Xu, C., Liu, Y., Liu, W., Bian, J., Wu, L., Li, Z., Chen, E., and Liu, T.-Y. Stock trend prediction with multi-granularity data: A contrastive learning approach with adaptive fusion. In *CIKM*, 2021.

Hyndman, R. J. and Athanasopoulos, G. *Forecasting: principles and practice*. OTexts, 2018.

Kollovieh, M., Ansari, A. F., Bohlke-Schneider, M., Zschiegner, J., Wang, H., and Wang, Y. Predict, refine, synthesize: Self-guiding diffusion models for probabilistic time series forecasting. In *In Proc. of NeurIPS*, 2023.

Lai, G., Chang, W., Yang, Y., and Liu, H. Modeling Long- and Short-Term Temporal Patterns with Deep Neural Networks. In *In Proc. of SIGIR*, pp. 95–104, 2018.

Li, Y., Lu, X., Wang, Y., and Dou, D. Generative Time Series Forecasting with Diffusion, Denoise, and Disentanglement. In *In Proc. of NeurIPS*, 2022.

Lim, B., Arik, S. Ö., Loeff, N., and Pfister, T. Temporal Fusion Transformers for Interpretable Multi-horizon Time Series Forecasting. *International Journal of Forecasting*, 2021.

LIU, M., Zeng, A., Chen, M., Xu, Z., LAI, Q., Ma, L., and Xu, Q. SCINet: Time Series Modeling and Forecasting with Sample Convolution and Interaction. In *In Proc. of NeurIPS*, 2022.

Liu, S., Yu, H., Liao, C., Li, J., Lin, W., Liu, A. X., and Dustdar, S. Pyraformer: Low-Complexity Pyramidal Attention for Long-Range Time Series Modeling and Forecasting. In *In Proc. of ICLR*, 2022.

Löning, M., Bagnall, A. J., Ganesh, S., Kazakov, V., Lines, J., and Király, F. J. Sktime: A Unified Interface for Machine Learning with Time Series. *CoRR*, abs/1909.07872, 2019. URL <http://arxiv.org/abs/1909.07872>.

Lv, Y., Duan, Y., Kang, W., Li, Z., and Wang, F.-Y. Traffic flow prediction with big data: A deep learning approach. *IEEE Transactions on Intelligent Transportation Systems*, 2014.

Makridakis, S. and Hibon, M. Arma models and the box-jenkins methodology. *Journal of forecasting*, 16(3):147–163, 1997.

Makridakis, S., Spiliotis, E., and Assimakopoulos, V. The m4 competition: 100,000 time series and 61 forecasting methods. *International Journal of Forecasting*, 36(1):54–74, 2020.

Makridakis, S., Spiliotis, E., and Assimakopoulos, V. The m5 competition: Background, organization, and implementation. *International Journal of Forecasting*, 38(4):1325–1336, 2022.

Matheson, J. E. and Winkler, R. L. Scoring Rules for Continuous Probability Distributions. *Management science*, 22(10):1087–1096, 1976.

Mudelsee, M. Trend analysis of climate time series: A review of methods. *Earth-science reviews*, 2019.

Nie, Y., Nguyen, N. H., Sinthong, P., and Kalagnanam, J. A Time Series is Worth 64 Words: Long-term Forecasting with Transformers. In *In Proc. of ICLR*, 2023.

Nielsen, F. On the Jensen–Shannon symmetrization of distances relying on abstract means. *Entropy*, 21(5):485, 2019.

Oguiza, I. tsai - A State-of-the-art Deep Learning Library for Time Series and Sequential Data. Github, 2022. URL <https://github.com/timeseriesAI/tsai>.

Orshkin, B. N., Carpow, D., Chapados, N., and Bengio, Y. N-BEATS: Neural basis expansion analysis for interpretable time series forecasting. In *In Proc. of ICLR*, 2020.

Papamakarios, G., Murray, I., and Pavlakou, T. Masked Autoregressive Flow for Density Estimation. In *In Proc. of NeurIPS*, pp. 2338–2347, 2017.

Rangapuram, S. S., Seeger, M. W., Gasthaus, J., Stella, L., Wang, Y., and Januschowski, T. Deep State Space Models for Time Series Forecasting. In *In Proc. of NeurIPS*, pp. 7796–7805, 2018.

Rasul, K., Seward, C., Schuster, I., and Vollgraf, R. Autoregressive Denoising Diffusion Models for Multivariate Probabilistic Time Series Forecasting. In *In Proc. of ICML*, pp. 8857–8868, 2021a.

Rasul, K., Sheikh, A., Schuster, I., Bergmann, U. M., and Vollgraf, R. Multivariate Probabilistic Time Series Forecasting via Conditioned Normalizing Flows. In *In Proc. of ICLR*, 2021b.

Salinas, D., Bohlke-Schneider, M., Callot, L., Medico, R., and Gasthaus, J. High-dimensional Multivariate Forecasting with Low-rank Gaussian Copula Processes. In *In Proc. of NeurIPS*, pp. 6824–6834, 2019.

Salinas, D., Flunkert, V., Gasthaus, J., and Januschowski, T. DeepAR: Probabilistic Forecasting with Autoregressive Recurrent Networks. *International Journal of Forecasting*, 36(3):1181–1191, 2020.

Smyl, S. A hybrid method of exponential smoothing and recurrent neural networks for time series forecasting. *International Journal of Forecasting*, 2020.

Tashiro, Y., Song, J., Song, Y., and Ermon, S. CSDI: Conditional Score-based Diffusion Models for Probabilistic Time Series Imputation. In *In Proc. of NeurIPS*, pp. 24804–24816, 2021.

Taylor, S. J. and Letham, B. Forecasting at Scale. *The American Statistician*, 2018.

Vaswani, A., Shazeer, N., Parmar, N., Uszkoreit, J., Jones, L., Gomez, A. N., Kaiser, L., and Polosukhin, I. Attention is All you Need. In *In Proc. of NeurIPS*, pp. 5998–6008, 2017.

Wang, H., Lei, Z., Zhang, X., Zhou, B., and Peng, J. A review of deep learning for renewable energy forecasting. *Energy Conversion and Management*, 2019.

Wang, X., Smith, K., and Hyndman, R. Characteristic-based Clustering for Time Series Data. *Data mining and knowledge Discovery*, 13:335–364, 2006.

Wen, R., Torkkola, K., Narayanaswamy, B., and Madeka, D. A Multi-horizon Quantile Recurrent Forecaster. *arXiv preprint arXiv:1711.11053*, 2017.

Wu, H., Xu, J., Wang, J., and Long, M. Autoformer: Decomposition Transformers with Auto-Correlation for Long-Term Series Forecasting. In *In Proc. of NeurIPS*, pp. 22419–22430, 2021.

Wu, H., Hu, T., Liu, Y., Zhou, H., Wang, J., and Long, M. TimesNet: Temporal 2D-Variation Modeling for General Time Series Analysis. In *In Proc. of ICLR*, 2023.

Zeng, A., Chen, M., Zhang, L., and Xu, Q. Are Transformers Effective for Time Series Forecasting? In *In Proc. of AAAI*, pp. 11121–11128, 2023.

Zhang, T., Zhang, Y., Cao, W., Bian, J., Yi, X., Zheng, S., and Li, J. Less is More: Fast Multivariate Time Series Forecasting with Light Sampling-Oriented MLP Structures. *arXiv preprint arXiv:2207.01186*, 2022.

Zhou, H., Zhang, S., Peng, J., Zhang, S., Li, J., Xiong, H., and Zhang, W. Informer: Beyond Efficient Transformer for Long Sequence Time-series Forecasting. In *In Proc. of AAAI*, pp. 11106–11115, 2021.

Zhou, T., Ma, Z., Wen, Q., Wang, X., Sun, L., and Jin, R. Fedformer: Frequency Enhanced Decomposed Transformer for Long-term Series Forecasting. In *In Proc. of ICMLg*, pp. 27268–27286, 2022.

A. More Details on ProbTS

A.1. Additional Related Work

Table 4 presents a comparative summary of our approach, which adopts an integrated perspective, and representative studies from the existing literature.

A.2. Time-series Forecasting Datasets

Table 5 provides a summary of the public datasets employed in our study. These datasets have been sourced from recent research studies in the field of deep time-series forecasting.

A.3. Data Visualization

To provide a more tangible understanding of the different forecasting scenarios, we visualize time-series segments from both short-term and long-term forecasting datasets. The segments’ window size is determined by the specific forecasting setup.

In Figure 4, we present samples extracted from short-term forecasting scenarios. At this scale, the series primarily exhibit local variations, and the compact window size often obscures pronounced seasonal or trending patterns. However, these short-term scenarios may reveal irregularly varied patterns, suggesting a more complex underlying data distribution.

On the contrary, Figure 5 illustrates long-term forecasting scenarios. With extended forecasting horizons, as showcased in datasets like Traffic, Electricity, and ETT, the series display more pronounced seasonality and trends. These characteristics render the series more regular patterns in the long-term scenarios.

It’s important to note that these visualizations are not selectively chosen or “cherry-picked”. We have depicted multiple time-series segments from various time steps, and the observed patterns remain consistent across these different instances.

A.4. Quantifying Trend and Seasonality Strengths

Based on the intuition obtained from data visualization, we would like to quantify the strengths of trend and seasonality for a time-series segment with a predefined window size (corresponding to the prediction horizon length). Then we can quantify the trend and seasonality strengths at the dataset level by averaging over all time-series segments of a dataset.

To quantify the strengths of trend and seasonality for a fixed-length time-series segment, we draw upon methodologies outlined in the work of (Wang et al., 2006). In particular, we employed a time series decomposition model expressed as:

$$y_t = T_t + S_t + R_t,$$

where T_t represents the smoothed trend component, S_t signifies the seasonal component, and R_t denotes the remainder component. In order to obtain each component, we followed the STL decomposition approach ⁴.

In the case of strongly trended data, the variation within the seasonally adjusted data should considerably exceed that of the remainder component. Consequently, the ratio $\text{Var}(R_t)/\text{Var}(T_t + R_t)$ is expected to be relatively small. As such, the measure of trend strength can be formulated as:

$$F_T = \max \left(0, 1 - \frac{\text{Var}(R_t)}{\text{Var}(T_t + R_t)} \right).$$

The quantified trend strength, ranging from 0 to 1, characterizes the degree of trend presence. Similarly, the evaluation of seasonal intensity employs the detrended data:

$$F_S = \max \left(0, 1 - \frac{\text{Var}(R_t)}{\text{Var}(S_t + R_t)} \right).$$

A series with F_S near 0 indicates minimal seasonality, while strong seasonality is indicated by F_S approaching 1 due to the considerably smaller variance of $\text{Var}(R_t)$ in comparison to $\text{Var}(S_t + R_t)$.

Tables 1 depict the results for each dataset. Notably, the ETT datasets and the Exchange dataset manifest conspicuous trends, whereas the Electricity, Solar, and Traffic datasets showcase marked seasonality. Additionally, the Exchange dataset stands out with distinctive features. Figure 5 also illustrates that with shorter prediction windows, the Exchange dataset sustains comparatively minor fluctuations, almost forming a linear trajectory. This enables effective forecasting through a straightforward batch mean approach. As the forecasting horizon extends, the dataset appears a more pronounced trend while retaining minimal seasonality.

⁴<https://otexts.com/fpp2/stl.html>

Table 4. We provide a concise comparison between the methodologies presented in this paper and those from two distinct research branches. The comparison is based on data scenarios (short-term versus long-term forecasting), primary evaluation metrics (point versus distributional forecasts), and key methodological choices (general or customized neural architecture designs, and autoregressive or non-autoregressive decoding schemes).

Method	Fore. Horizon		Metrics		Arch. Design		Dec. Scheme	
	Short	Long	Point	Distr.	General	Customized	Autoreg.	Non-autoreg.
N-BEATS (Oreshkin et al., 2020)	✗	✓	✓	✗	✗	✓	✗	✓
Autoformer (Wu et al., 2021)	✗	✓	✓	✗	✗	✓	✗	✓
Informer (Zhou et al., 2021)	✗	✓	✓	✗	✗	✓	✗	✓
Pyraformer (Liu et al., 2022)	✗	✓	✓	✗	✗	✓	✗	✓
N-HiTS (Challu et al., 2023)	✗	✓	✓	✗	✗	✓	✗	✓
LTSF-Linear (Zeng et al., 2023)	✗	✓	✓	✗	✗	✓	✗	✓
PatchTST (Nie et al., 2023)	✗	✓	✓	✗	✗	✓	✗	✓
TimesNet (Wu et al., 2023)	✓	✓	✓	✗	✗	✓	✗	✓
DeepAR (Salinas et al., 2020)	✓	✗	✗	✓	✓	✗	✓	✗
GP-copula (Salinas et al., 2019)	✓	✗	✗	✓	✓	✗	✓	✗
LSTM NVP (Rasul et al., 2021b)	✓	✗	✗	✓	✓	✗	✓	✗
LSTM MAF (Rasul et al., 2021b)	✓	✗	✗	✓	✓	✗	✓	✗
Trans MAF (Rasul et al., 2021b)	✓	✗	✗	✓	✓	✗	✓	✗
TimeGrad (Rasul et al., 2021a)	✓	✗	✗	✓	✓	✗	✓	✗
CSDI (Tashiro et al., 2021)	✓	✗	✗	✓	✗	✓	✗	✓
SPD (Bilos et al., 2023)	✓	✗	✗	✓	✓	✗	✗	✓
TSDiff (Kolloviev et al., 2023)	✓	✗	✗	✓	✗	✓	✗	✓
This Paper	✓	✓	✓	✓	✓	✓	✓	✓

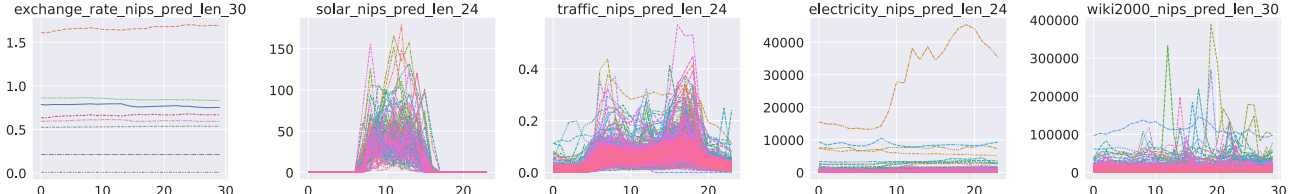


Figure 4. We have sampled and visualized multiple time-series segments from the short-term forecasting datasets. The size of the segment window is set equal to the prediction horizon.

A.5. Quantifying Data Distribution Complexity

To differentiate between methods optimized for point or distributional forecasts, we aim to quantify the complexity of data distribution within a time-series segment whose window size equals the prediction horizon length. We propose that assessing non-Gaussianity, i.e., how closely the distribution of time-series values within that window resembles a Gaussian distribution, could serve as a meaningful measure. This is because point forecasting methods, optimized with mean squared loss, are essentially equivalent to probabilistic counterparts that include a Gaussian output head and employ maximum a posteriori estimation. This suggests that point forecasting methods inherently assume that time-series values adhere to a Gaussian distribution. In contrast, advanced probabilistic methods, which do not make prior

assumptions about data distribution, can adapt to complex data distributions in a data-driven manner.

Hence, we use the Jensen–Shannon divergence (Nielsen, 2019) to measure the similarity between the actual value distribution of a time-series segment and a Gaussian distribution fitted to the observed values. Short-term datasets used a window size of 30, while long-term datasets used a size of 336. By averaging the calculated divergence values across all time-series segments of a dataset, we obtain a dataset-level measure of non-Gaussianity. A larger divergence value indicates a larger deviation from a Gaussian distribution in the data.

Table 5. Dataset Summary.

Horizon	Dataset	#var.	range	freq.	timesteps	Description
Long-term	ETTh1/h2	7	\mathbb{R}^+	H	17,420	Electricity transformer temperature per hour
	ETTm1/m2	7	\mathbb{R}^+	15min	69,680	Electricity transformer temperature every 15 min
	Electricity	321	\mathbb{R}^+	H	26,304	Electricity consumption (Kwh)
	Traffic	862	(0,1)	H	17,544	Road occupancy rates
	Exchange	8	\mathbb{R}^+	Busi. Day	7,588	Daily exchange rates of 8 countries
	ILI	7	(0,1)	W	966	Ratio of patients seen with influenza-like illness
	Weather	21	\mathbb{R}^+	10min	52,696	Local climatological data
Short-term	Exchange	8	\mathbb{R}^+	Busi. Day	6,071	Daily exchange rates of 8 countries
	Solar	137	\mathbb{R}^+	H	7,009	Solar power production records
	Electricity	370	\mathbb{R}^+	H	5,833	Electricity consumption
	Traffic	963	(0,1)	H	4,001	Road occupancy rates
	Wikipedia	2,000	N	D	792	Page views of 2000 Wikipedia pages

A.6. Evaluation Metrics

In ProbTS, we integrate an extensive variety of metrics that take into account both point and distributional forecasts, thereby providing a comprehensive and multifaceted assessment of forecasting models.

A.6.1. METRICS FOR POINT FORECASTS

Mean Absolute Error (MAE) The Mean Absolute Error (MAE) quantifies the average absolute deviation between the forecasts and the true values. Since it averages the absolute errors, MAE is robust to outliers. Its mathematical formula is given by:

$$\text{MAE} = \frac{1}{K \times T} \sum_{i=1}^K \sum_{t=1}^T |x_{i,t} - \hat{x}_{i,t}|,$$

where K is the number of variates, L is the length of series, $x_{i,t}$ and $\hat{x}_{i,t}$ denotes the ground-truth value and the predicted value, respectively. For multivariate time series, we also provide the aggregated version:

$$\text{MAE}_{\text{sum}} = \frac{1}{T} \sum_{t=1}^T |x_t^{\text{sum}} - \hat{x}_t^{\text{sum}}|,$$

where x_t^{sum} and \hat{x}_t^{sum} are the summation across the dimension K of $x_{i,t}$ and $\hat{x}_{i,t}$, respectively.

Normalized Mean Absolute Error (NMAE) The Normalized Mean Absolute Error (NMAE) is a normalized version of the MAE, which is dimensionless and facilitates the comparability of the error magnitude across different datasets or scales. The mathematical representation of NMAE is given by:

$$\text{NMAE} = \frac{1}{K \times T} \sum_{i=1}^K \sum_{t=1}^T \frac{|x_{i,t} - \hat{x}_{i,t}|}{|x_{i,t}|}.$$

Its aggregated version is:

$$\text{NMAE}_{\text{sum}} = \frac{1}{T} \sum_{t=1}^T \frac{|x_t^{\text{sum}} - \hat{x}_t^{\text{sum}}|}{|x_t^{\text{sum}}|}.$$

Mean Squared Error (MSE) The Mean Squared Error (MSE) is a quantitative metric used to measure the average squared difference between the observed actual value and forecasts. It is defined mathematically as follows:

$$\text{MSE} = \frac{1}{K \times T} \sum_{i=1}^K \sum_{t=1}^L (x_{i,t} - \hat{x}_{i,t})^2.$$

For multivariate time series, we also provide the aggregated version:

$$\text{MSE}_{\text{sum}} = \frac{1}{T} \sum_{t=1}^L (x_t^{\text{sum}} - \hat{x}_t^{\text{sum}})^2.$$

Normalized Root Mean Squared Error (NRMSE) The Normalized Root Mean Squared Error (NRMSE) is a normalized version of the Root Mean Squared Error (RMSE), which quantifies the average squared magnitude of the error between forecasts and observations, normalized by the expectation of the observed values. It can be formally written as:

$$\text{NRMSE} = \frac{\sqrt{\frac{1}{K \times T} \sum_{i=1}^K \sum_{t=1}^L (x_{i,t} - \hat{x}_{i,t})^2}}{\frac{1}{K \times T} \sum_{i=1}^K \sum_{t=1}^T |x_{i,t}|}.$$

For multivariate time series, we also provide the aggregated version:

$$\text{NRMSE}_{\text{sum}} = \frac{\sqrt{\frac{1}{T} \sum_{t=1}^L (x_t^{\text{sum}} - \hat{x}_t^{\text{sum}})^2}}{\frac{1}{T} \sum_{t=1}^T |x_t^{\text{sum}}|}.$$

A.6.2. METRICS FOR DISTRIBUTIONAL FORECASTS

Continuous Ranked Probability Score (CRPS) The Continuous Ranked Probability Score (CRPS) (Matheson & Winkler, 1976) quantifies the agreement between a cumulative distribution function (CDF) F and an observation x , represented as:

$$\text{CRPS} = \int_{\mathbb{R}} (F(z) - \mathbb{I}\{x \leq z\})^2 dz,$$

where $\mathbb{I}x \leq z$ denotes the indicator function, equating to one if $x \leq z$ and zero otherwise.

Being a proper scoring function, CRPS reaches its minimum when the predictive distribution F coincides with the data distribution. When using the empirical CDF of F , denoted as $\hat{F}(z) = \frac{1}{n} \sum_{i=1}^n \mathbb{I}\{X_i \leq z\}$, where n represents the number of samples $X_i \sim F$, CRPS can be precisely calculated from the simulated samples of the conditional distribution $p_{\theta}(x_t | \mathbf{h}_t)$. In our practice, 100 samples are employed to estimate the empirical CDF.

For multivariate time series, the aggregate CRPS, denoted as CRPS_{sum} , is derived by summing across the K time series, both for the ground-truth data and sampled data, and subsequently averaging over the forecasting horizon. Formally, it is represented as:

$$\text{CRPS}_{\text{sum}} = \mathbb{E}_t \left[\text{CRPS} \left(\hat{F}_{\text{sum}}(t), \sum_{i=1}^K x_{i,l}^0 \right) \right].$$

A.7. Implementation Details

ProbTS was developed using PyTorch Lightning (Falcon & The PyTorch Lightning team, 2019). During training, we sampled 100 batches per epoch and limited training to 50 epochs, using the CRPS metric for checkpointing. All experiments employed the Adam optimizer and were run on single NVIDIA Tesla V100 GPUs with CUDA 11.3. To enable evaluation of distribution-level metrics, we conducted 100 samplings to calculate metrics on the test set.

Following the most commonly adopted settings (Zeng et al., 2023; Nie et al., 2023; Wu et al., 2023), in the long-term forecasting context, all of the models are following the same experimental setup with prediction length $T \in \{24, 36, 48, 60\}$ for ILI dataset and $T \in \{96, 192, 336, 720\}$ for other datasets. Note that the look-back window here is 96 for all the models, to ensure a fair comparison. In the short-term forecasting context, the length of the lookback window is the same as the forecasting horizons, which are 30 for Exchange-S dataset and Wikipedia-S dataset, and 24 for the rest, the same as (Salinas et al., 2019).

Hyper-parameter Tuning For a fair comparison, we conducted a comprehensive grid search for critical hyperparameters across all models in this study. Table 6 details the

shared hyperparameters tuned within the ProbTS pipeline, along with those kept constant. Due to the vast array of model-specific hyperparameters, we present an example configuration in Table 7. Complete hyperparameter configurations for each model, identified through this process, will be made available in a public GitHub repository for transparency and reproducibility.

Table 6. Hyper-parameters values fixed or range searched in hyper-parameter tuning.

Hyper-parameter	Value or Range Searched
learning rate	[1e-4, 1e-3, 1e-2]
dropout	[0, 0.1, 0.2]
batch_size	[8, 16, 32, 64]
use_lags	[True, False]
use_feat_idx_emb	[True, False]
use_time_feat	[True, False]
autoregressive	[True, False]
scaler	[Standard, Scaling, None]
limit_train_batches	100
num_samples	100
quantiles_num	20

B. Additional Results and Experiments

B.1. Impact of Data Scale

To further explore critical characteristics of time-series forecasting, we have examined the correlation between model performance gains, relative to the baseline model (GRU), and dataset dimensions, length, and volume (see Table 8). However, our analysis does not identify a significant correlation between these factors and model performance.

B.2. Statistical and Gradient Boosting Decision Tree Baselines

To enhance the empirical robustness of our study, we integrate classical statistical models, including ARIMA (Makridakis & Hibon, 1997) and ETS (Hyndman & Athanasopoulos, 2018), along with the Gradient Boosting Decision Tree (GBDT) model, XGBoost, into the ProbTS framework. The results in Table 9 clearly demonstrate the superior performance of deep learning methods over simple statistical baselines, emphasizing the importance of capturing non-linear dependencies for accurate forecasts. Notably, ARIMA and ETS exhibit varied performance across different data characteristics. ARIMA struggles with datasets like Solar, characterized by weak trending and strong seasonality, while ETS shows better adaptability. Conversely, in cases of strong trending and weak seasonality, as observed in the 'Wikipedia' dataset, ARIMA significantly outperforms ETS.

Utilizing the implementation from (Elsayed et al., 2021), we

Table 7. Hyperparameter settings for Electricity-S dataset.

Model	Hyperparameter
DLinear	learning_rate=0.01, kernel_size=3, f_hidden_size=40
PatchTST	learning_rate=0.0001, stride=3, patch_len=6, n_layers=3, n_heads=8, dropout=0.1, kernel_size=3, f_hidden_size=32
TimesNet	learning_rate=0.001, n_layers=2, num_kernels=6, top_k=5, f_hidden_size=64, d_ff=64
GRU NVP	learning_rate=0.001, f_hidden_size=40, num_layers=2, n_blocks=3, hidden_size=100, conditional_length=200
GRU MAF	learning_rate=0.001, f_hidden_size=40, num_layers=2, n_blocks=4, hidden_size=100, conditional_length=200
Trans MAF	learning_rate=0.001, f_hidden_size=32, num_heads=8, n_blocks=4, hidden_size=100, conditional_length=200
TimeGrad	learning_rate=0.001, f_hidden_size=128, num_layers=4, conditional_length=100, beta_end=0.1, diff_steps=100
CSDI	learning_rate=0.001, channels=64, emb_time_dim=128, emb_feature_dim=16, num_steps=50, num_heads=8, n_layers=4

Table 8. The correlation coefficient between the data volume and the relative performance improvement compared to the baseline model (GRU).

Model	DLinear		PatchTST		GRU NVP		TimeGrad		CSDI	
	CRPS	NMAE	CRPS	NMAE	CRPS	NMAE	CRPS	NMAE	CRPS	NMAE
# Var.	0.2422	0.2422	-0.2676	-0.2676	-0.1856	-0.2136	-0.1665	-0.1793	-0.2315	-0.2592
# Total timestep	-0.1422	-0.1422	0.3821	0.3821	0.3072	0.3329	0.2860	0.2971	0.3542	0.3826
# Var. × Timestep	0.0162	0.0162	0.0166	0.0166	-0.0068	-0.0011	0.0082	0.0117	-0.0053	-0.0133

find that XGBoost competes well, even surpassing neural network models in certain scenarios. However, for datasets with more complex distributions like 'Solar' and 'Electricity,' advanced probabilistic estimation methods demonstrate a substantial advantage over traditional learning methods and point estimation techniques. This highlights the adaptability and strength of advanced probabilistic methods in handling intricate forecasting scenarios.

B.3. Experiments on Univariate Datasets

In pursuit of a comprehensive analysis spanning univariate and multivariate scenarios, we examined a subset of M4 (Makridakis et al., 2020), M5 (Makridakis et al., 2022), and TOURISM datasets (Athanasopoulos et al., 2011)—crucial datasets for univariate time-series forecasting. Table 10 provides a quantitative assessment of the intrinsic characteristics of these new datasets, focusing on trending strength, seasonality, and data distribution complexity, as detailed in our paper. Notably, these datasets, except for M4-Daily may exhibit fewer seasonal patterns, do not introduce particularly unique characteristics.

Table 11 presents experimental results for representative methods, consistent with our initial observations. Probabilistic estimation methods like GRU NVP and TimeGrad excel on datasets with complex distributions (e.g., M4-Weekly and M5), while simpler point forecasting methods such as DLinear and PatchTST perform well on datasets with relatively simple data distribution, like TOURISM-Monthly. Both

autoregressive and non-autoregressive decoding schemes show comparable performance in short-term forecasting, as discussed in the main paper.”

B.4. Experiments on Synthetic Datasets

To enhance the rigor of the insights presented, we employ synthetic datasets created with the GluonTS library⁵, encompassing a baseline dataset and variants with pronounced trends, strong seasonality, and complex data distribution (see Table 12). Specifically, we generate these datasets by superimposing four components - trend, seasonality, noise, and anomaly - each with adjustable intensity parameters. The seasonality component is defined by period hyper-parameters and intensity coefficients; the trend by slope intensity; the noise by Gaussian distribution sampling with adjustable intensity; and the anomaly by occurrence probability and maximum intensity.

Subsequent experiments on these synthetic datasets (refer to Table 13), using representative models, validate the empirical findings established on other datasets with ProbTS. Key observations include the declining performance of autoregressive decoding models, such as TimeGrad, in the presence of increasing trends, improved performance for models using autoregressive decoding with intensifying seasonality, and the competitive performance of probabilistic

⁵https://ts.gluon.ai/stable/tutorials/data_manipulation/index.html

Table 9. Results of statistical models and GBDT baseline on short-term forecasting datasets.

Model	Exchange Rate		Solar		Electricity		Traffic		Wikipedia	
	CRPS	NMAE								
ARIMA	0.009	0.009	1.000	1.000	0.164	0.164	0.461	0.461	0.348	0.348
ETS	0.011	0.011	0.580	0.580	0.121	0.121	0.413	0.413	0.685	0.685
ETS-prob	0.008	0.011	0.795	0.695	0.123	0.129	0.380	0.433	0.625	0.697
XGBoost	0.011	0.011	0.599	0.599	0.074	0.074	0.196	0.196	-	-
DLinear	0.012 _{.001}	0.012 _{.001}	0.547 _{.009}	0.547 _{.009}	0.095 _{.006}	0.095 _{.006}	0.273 _{.012}	0.273 _{.012}	1.046 _{.037}	1.046 _{.037}
PatchTST	<u>0.010_{.000}</u>	0.010_{.000}	0.496 _{.002}	0.496 _{.002}	0.076 _{.001}	0.076 _{.001}	0.202 _{.001}	0.202 _{.001}	<u>0.257_{.001}</u>	0.257_{.001}
TimesNet	0.011 _{.001}	0.011 _{.001}	0.507 _{.019}	0.507 _{.019}	0.071 _{.002}	0.071 _{.002}	0.205 _{.002}	0.205 _{.002}	0.304 _{.002}	0.304 _{.002}
GRU NVP	0.016 _{.003}	0.020 _{.003}	0.396 _{.021}	0.507 _{.022}	0.055 _{.002}	0.073 _{.003}	0.161 _{.006}	0.203 _{.009}	0.282 _{.003}	0.330 _{.003}
GRU MAF	0.015 _{.001}	0.020 _{.001}	0.386 _{.026}	0.492 _{.027}	0.051 _{.001}	0.067 _{.001}	0.131 _{.006}	0.165 _{.009}	0.281 _{.004}	0.337 _{.005}
Trans MAF	0.011 _{.001}	0.014 _{.001}	0.400 _{.022}	0.503 _{.022}	0.054 _{.004}	0.071 _{.005}	0.129_{.004}	0.165_{.006}	0.289 _{.008}	0.344 _{.008}
TimeGrad	0.011 _{.001}	0.014 _{.002}	0.359_{.011}	0.445_{.023}	0.052 _{.001}	<u>0.067_{.001}</u>	0.164 _{.091}	0.201 _{.115}	0.272 _{.008}	0.327 _{.011}
CSDI	0.008_{.000}	<u>0.011_{.000}</u>	0.366 _{.005}	0.484 _{.008}	0.050_{.001}	0.065_{.001}	0.146 _{.012}	0.176 _{.013}	0.219_{.006}	<u>0.259_{.009}</u>

Table 10. Quantitative assessment of the intrinsic characteristics of the univariate datasets. The JS Div. denotes Jensen–Shannon divergence, where a lower score indicates closer approximations to a Gaussian distribution.

Dataset	M4-Weekly	M4-Daily	M5	TOURISM-Monthly
Trend F_T	0.7677	0.9808	0.3443	0.7979
Seasonality F_S	0.3401	0.0467	0.2480	0.6826
JS Div.	0.5106	0.4916	0.6011	0.3291

methods like CSDI in handling more complex data distributions.

B.5. Case Study

To intuitively demonstrate the distinct characteristics of point and probabilistic estimations, a case study was conducted on short-term datasets. Figure 6 illustrates that point estimation yields single-valued, deterministic estimates, in contrast to probabilistic methods, which model continuous data distributions as depicted in Figure 7. This modeling of data distributions captures the uncertainty in forecasts, aiding decision-makers in fields such as weather and finance to make more informed choices. It is also observed that while both methods align well with ground truth values in short-term forecasting datasets, they struggle to accurately capture outliers, particularly noted in the Wikipedia dataset.

B.6. Model Efficiency

For reference, detailed results regarding memory usage and time efficiency for five representative models on long-term forecasting datasets are provided here. Table 14 displays the computation memory of various models with a forecasting horizon set to 96. Additionally, Table 15 compares the inference time of these models on long-term forecasting datasets, illustrating the impact of changes in the forecasting horizon.

B.7. Further Discussion on Cross-channel Interactions

We compile a summary table (Table 16) delineating how models from each branch address the multivariate aspect. Despite a thorough investigation, we have not identified a clear pattern linking the modeling of cross-channel interactions to overall model performance. A notable trend is the prevalent use of a channel-mixing approach in most studies. However, findings are diverse; models like DLinear and PatchTST suggest that processing channels independently can yield superior results, while others like CSDI indicate that explicit modeling of cross-channel interactions offers significant advantages. This diversity underscores the ongoing exploration of the impact of cross-channel interactions on forecasting performance.

Table 11. Results on M4, M5, and TOURISM datasets. We utilize a lookback window of 3H, with 'H' denoting the forecasting horizon.

Model	DLinear		PatchTST		GRU NVP		TimeGrad	
	CRPS	NMAE	CRPS	NMAE	CRPS	NMAE	CRPS	NMAE
M4-Weekly	0.081	0.081	0.089	0.089	0.066	0.077	0.055	0.065
M4-Daily	0.034	0.034	0.035	0.035	0.030	0.038	0.026	0.032
M5	0.891	0.891	0.898	0.898	0.679	0.864	-	-
TOURISM-Monthly	0.168	0.168	0.136	0.136	0.171	0.223	0.152	0.191

Table 12. Quantitative assessment of intrinsic characteristics for synthetic datasets. The JS Div denotes Jensen–Shannon divergence, where a lower score indicates closer approximations to a Gaussian distribution.

Dataset	Normal	Strong Trend	Strong Seasonality	Complex Distribution
Trend F_T	0.105	0.554	0.105	0.064
Seasonality F_S	0.302	0.302	0.791	0.190
JS Div.	0.261	0.248	0.272	0.469

Table 13. Results on synthetic datasets. The look-back window and forecasting horizon are 30.

Model	Normal		Strong Trend		Strong Seasonality		Complex Distribution	
	CRPS	NMAE	CRPS	NMAE	CRPS	NMAE	CRPS	NMAE
DLinear	0.013	0.013	0.001	0.001	0.014	0.014	0.301	0.301
PatchTST	0.012	0.012	0.001	0.001	0.012	0.012	0.275	0.275
TimeGrad	0.024	0.032	0.042	0.048	0.022	0.028	0.283	0.338
CSDI	0.013	0.014	0.010	0.007	0.020	0.027	0.269	0.301

Table 14. Computation memory. The batch size is 1 and the prediction horizon is set to 96.

Metric	Dataset	DLinear	PatchTST	LSTM NVP	TimeGrad	CSDI
NPARAMS (MB)	ETTm1	0.075	2.145	1.079	1.233	1.720
	Electricity	0.076	2.146	3.680	3.472	1.370
	Traffic	0.078	2.149	15.926	8.298	1.390
	Weather	0.075	2.145	3.085	0.574	1.721
	Exchange	0.075	0.135	1.979	0.488	1.720
Max GPU Mem. (GB)	ETTm1	0.002	0.009	0.010	0.012	0.027
	Electricity	0.060	0.068	0.129	0.128	1.411
	Traffic	0.161	0.168	0.361	0.333	9.102
	Weather	0.004	0.012	0.021	0.012	0.070
	Exchange	0.002	0.002	0.013	0.008	0.030

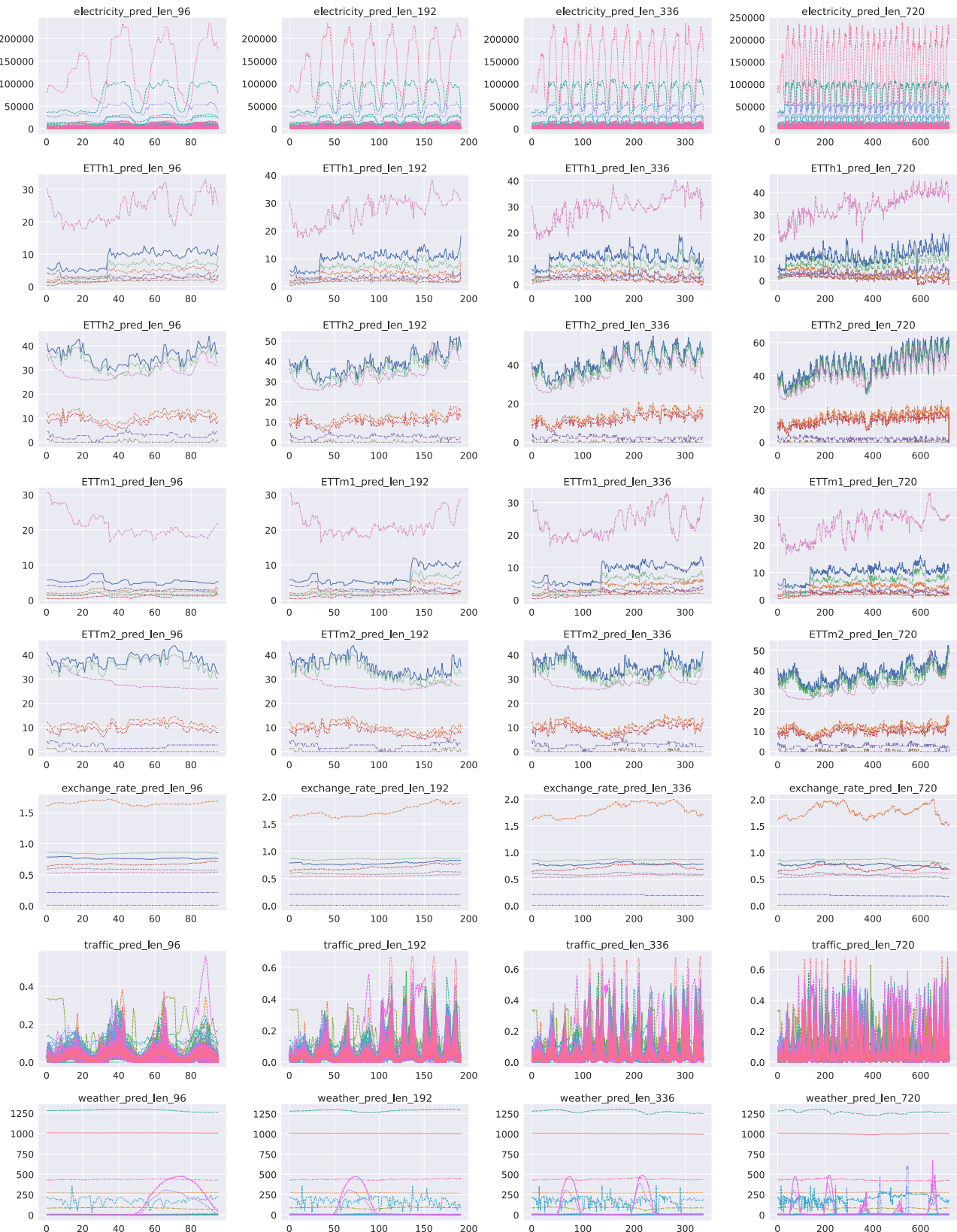


Figure 5. We have also sampled and visualized multiple time-series segments from the long-term forecasting datasets, where the size of the segment window matches the prediction horizon.

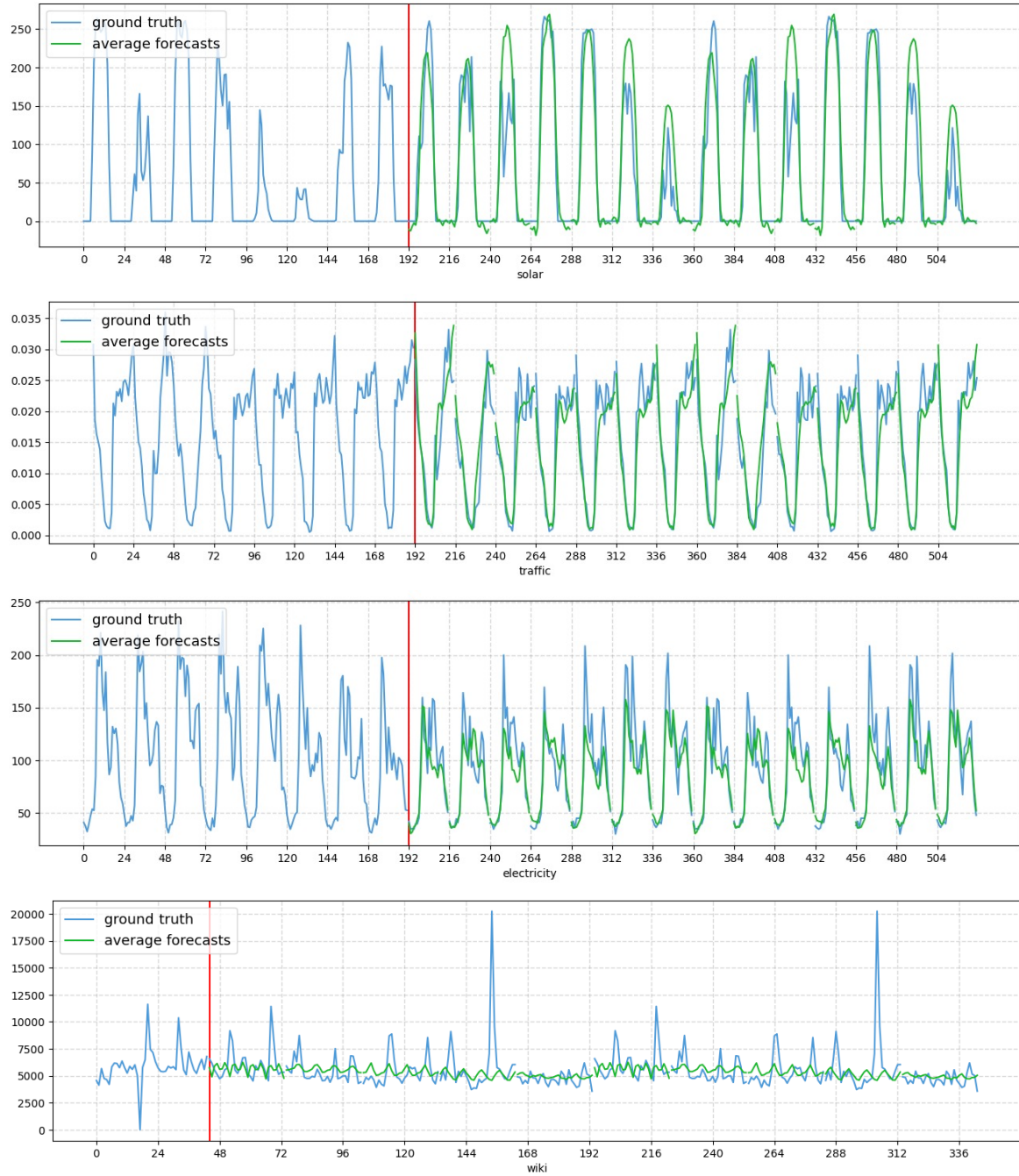


Figure 6. Point forecasts from the PatchTST model and the ground-truth value on short-term forecasting datasets.

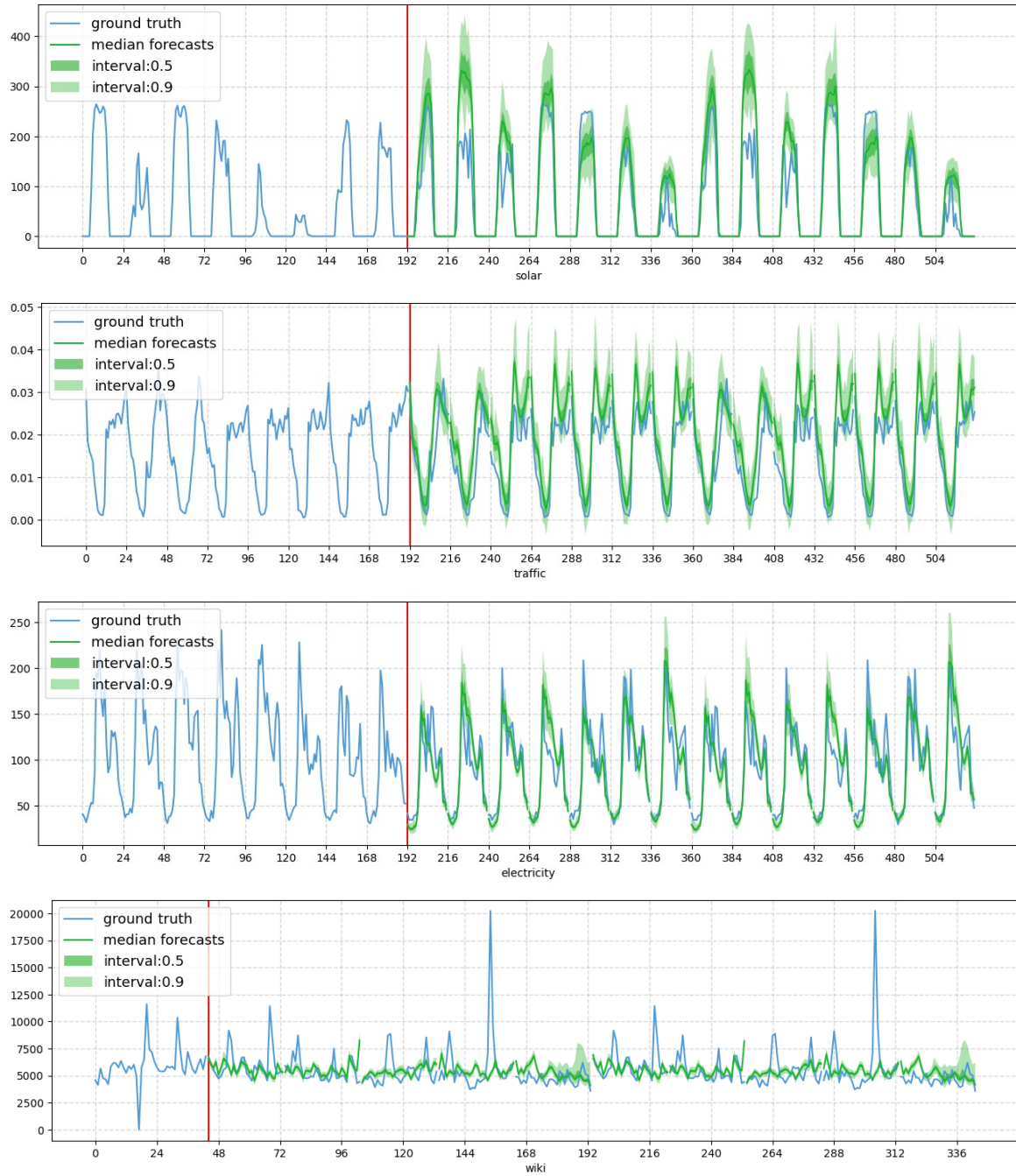


Figure 7. Forecasting intervals from the TimeGrad model and the ground-truth value on short-term forecasting datasets.

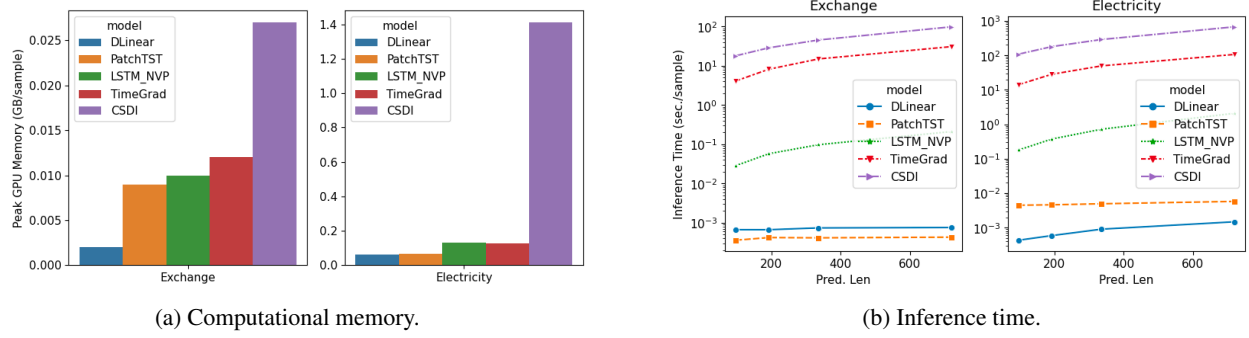


Figure 8. Comparison of computational efficiency. The forecasting horizon is set to 96 for calculating memory usage.

Table 15. Comparison of inference time (sec./sample).

Model	pred len	DLinear	PatchTST	LSTM_NVP	TimeGrad	CSDI
ETTm1	96	0.0003 ± 0.0000	0.0003 ± 0.0000	0.0352 ± 0.0007	4.1067 ± 0.0504	16.3280 ± 0.0747
	192	0.0003 ± 0.0000	0.0003 ± 0.0000	0.0697 ± 0.0020	7.8979 ± 0.0403	25.8378 ± 0.3124
	336	0.0003 ± 0.0000	0.0003 ± 0.0000	0.1221 ± 0.0044	13.6197 ± 0.1023	39.8832 ± 0.2157
	720	0.0004 ± 0.0000	0.0003 ± 0.0000	0.2603 ± 0.0020	28.6074 ± 1.1346	86.1862 ± 0.1863
Electricity	96	0.0004 ± 0.0000	0.0045 ± 0.0001	0.1783 ± 0.0006	13.8439 ± 0.0054	388.3150 ± 0.2155
	192	0.0006 ± 0.0000	0.0046 ± 0.0000	0.3700 ± 0.0010	27.6683 ± 0.0368	659.4284 ± 0.2003
	336	0.0008 ± 0.0000	0.0049 ± 0.0000	0.7157 ± 0.0028	48.4456 ± 0.0279	-
	720	0.0015 ± 0.0000	0.0057 ± 0.0000	2.0785 ± 0.0186	104.1473 ± 0.1465	-
Traffic	96	0.0010 ± 0.0001	0.0102 ± 0.0000	0.3695 ± 0.0022	31.7644 ± 0.0101	-
	192	0.0013 ± 0.0000	0.0106 ± 0.0000	0.8287 ± 0.0094	63.5832 ± 0.0060	-
	336	0.0020 ± 0.0000	0.0114 ± 0.0001	1.6945 ± 0.0026	111.4147 ± 0.0169	-
	720	0.0039 ± 0.0000	0.0137 ± 0.0000	5.0963 ± 0.0018	258.1274 ± 0.6088	-
Weather	96	0.0002 ± 0.0000	0.0004 ± 0.0000	0.0800 ± 0.0016	4.1261 ± 0.0812	37.8984 ± 0.0782
	192	0.0003 ± 0.0000	0.0004 ± 0.0000	0.1568 ± 0.0008	8.2913 ± 0.5544	62.0223 ± 0.2329
	336	0.0003 ± 0.0000	0.0004 ± 0.0000	0.2482 ± 0.0297	14.2391 ± 0.4891	96.8704 ± 0.2258
	720	0.0003 ± 0.0000	0.0005 ± 0.0000	0.5447 ± 0.0249	29.4407 ± 0.3519	216.6044 ± 0.4253
Exchange	96	0.0006 ± 0.0000	0.0004 ± 0.0000	0.0284 ± 0.0001	4.1069 ± 0.0981	17.8655 ± 0.1282
	192	0.0007 ± 0.0000	0.0004 ± 0.0000	0.0563 ± 0.0008	8.1576 ± 0.0911	28.5456 ± 0.0873
	336	0.0007 ± 0.0000	0.0004 ± 0.0000	0.0966 ± 0.0007	14.4593 ± 0.4466	44.9733 ± 0.3820
	720	0.0007 ± 0.0000	0.0004 ± 0.0000	0.2085 ± 0.0046	30.1443 ± 0.5378	97.7417 ± 0.2606
ILI	24	0.0002 ± 0.0000	0.0008 ± 0.0001	0.0080 ± 0.0001	1.0427 ± 0.0190	12.4038 ± 0.1681
	192	0.0002 ± 0.0000	0.0008 ± 0.0000	0.0121 ± 0.0003	1.5762 ± 0.0282	12.7187 ± 0.1344
	336	0.0002 ± 0.0000	0.0008 ± 0.0000	0.0155 ± 0.0002	2.1344 ± 0.0660	12.7386 ± 0.1868
	720	0.0002 ± 0.0000	0.0008 ± 0.0000	0.0196 ± 0.0004	2.5787 ± 0.0594	12.5407 ± 0.0481

Table 16. Summary of how existing models handle multivariate time series.

Model	Research branch	Process channels independently
Customized neural architectures	N-BEATS (Oreshkin et al., 2020)	✓
	N-HiTS (Challu et al., 2023)	✓
	Autoformer (Wu et al., 2021)	✗
	Informer (Zhou et al., 2021)	✗
	LTSF-Linear (Zeng et al., 2023)	✗/✓
	PatchTST (Nie et al., 2023)	✗/✓
	TimesNet (Wu et al., 2023)	✗
Probabilistic estimation	DeepAR (Salinas et al., 2020)	✓
	GP-copula (Salinas et al., 2019)	✗
	LSTM NVP (Rasul et al., 2021b)	✗
	LSTM MAF (Rasul et al., 2021b)	✗
	Trans MAF (Rasul et al., 2021b)	✗
	TimeGrad (Rasul et al., 2021a)	✗
	CSDI (Tashiro et al., 2021)	✗
	SPD (Bilos et al., 2023)	✗